ELSEVIER

Materials Science and Engineering B 139 (2007) 226–231

MATERIALS SCIENCE & ENGINEERING B

www.elsevier.com/locate/mseb

Ionic conductivity of metallic cations encapsulated in zeolite Y and mordenite

K. Ben Saad [a,*], H. Hamzaoui [b], M.M. Mohamed [c]

[a] *Institut National de Recherche Scientifique et Technique, Laboratoire de Photovoltaïque et des Semi-conducteurs, BP 95, 2050 Hammam-Lif, Tunisia*
[b] *Institut National de Recherche Scientifique et Technique, Laboratoire des procédés chimique, BP 95, 2050 Hammam-Lif, Tunisia*
[c] *Departement of Chemistry, Faculty of Science, Benha University, Benha, Egypt*

Received 23 November 2005; received in revised form 12 February 2007; accepted 27 February 2007

Abstract

Ionic conductivity curves of powder zeolite Y and mordenite encapsulating initially cobalt, nickel or copper cations, was determined by the shift of the cut-off frequency of the imaginary part of their complex impedances for temperatures lower than 650 °C. We have shown that zeolite Y containing nickel cations has 1 eV as activation energy in the range of temperature [530–600 °C], and with the addition of a small quantity of lithium its conductivity curve has undergone a shift towards lower energies. In addition, in the range [445–600 °C], cobalt cations in zeolite Y have a conductivity coefficient in the vicinity of [0.89–2.77] $\times 10^{-6}\ \Omega^{-1}\ m^{-1}$ and activation energy 0.88 eV. With the lithium addition these values was changed, respectively, to [0.13–1.44] $\times 10^{-6}\ \Omega^{-1}\ m^{-1}$ and 1 eV in the range [405–600 °C].

The same observations were obtained for copper cations in mordenite. The conductivity of this sample was changed from [1.12–4.25] $\times 10^{-6}\ \Omega^{-1}\ m^{-1}$ in the narrow range [550–650 °C] to [0.06–4.04] $\times 10^{-6}\ \Omega^{-1}\ m^{-1}$ in the wider one [370–650 °C] after lithium addition.

Keywords: Zeolite Y; Mordenite; Impedance; Conductivity; Cobalt; Nickel; Copper; Lithium

1. Introduction

Zeolites have attracted considerable attention due to their potential applications in many fields. We give in this section a short outline of some important studies and their impact on everyday life. First of all, zeolites can carry the dual function of separator and catalyst [1–5]. They were used like gas [6–9], pH [10] or humidity sensors [11]. Cylindrical zeolite L crystals filled with dye molecules can transfer electronic excitation and challenges for developing new photonic devices for solar energy conversion and storage [12]. With an aim of employing zeolites as gas storage materials, investigation of hydrogen adsorption by number of zeolites are in progress. The largest uptake of hydrogen was found to be at low temperatures [13]. Due to presence of carbon monoxide in hydrogen gas, corrosion in the fuel cells electrodes may happen and reduces its power output. To avoid this problem some researchers employed A-zeolites with noble metals to purify hydrogen gas [14]. Desulphurization of transportation fuels is the point of interest of some other authors; they proved that it may be accomplished by zeolites at ambient temperature [15]. In addition, the formation of molecular clusters entrapped in the pores of Y-zeolite has been investigated using FTIR spectroscopy and a blue shift of the carbon oxide bands in Y-zeolite has been observed during the sodium cation exchange by other cations [16]. Intense effort were also provided to prepare zeolite monolayer films with controlled orientation, these samples are favorable for molecular diffusion and may have a potential application for biosensor manufacture [17].

Combined with cobalt oxide, zeolites may be used as materials for adsorption and conversion of environment pollutants [18]. Modified by manganese or lanthanum or mixture of both, zeolites present photocatalytic and decolorization activities [19]. The investigation of the forms and dimensions of the zeolite films cavities may contribute to the development of the low-*k* thin films necessary for development of the future microprocessors [20]. Previous study has also proved that the insertion of the ZSM-5 zeolite in compressed lead-acid batteries has given improvements to its electrical performances [21]. Other authors have enriched these experimental studies and have proposed

* Corresponding author. Tel.: +216 71 430 160; fax: +216 71 430 934.
E-mail address: BenSaadKhaled2005@yahoo.fr (K. Ben Saad).

0921-5107/$ – see front matter © 2007 Elsevier B.V. All rights reserved.
doi:10.1016/j.mseb.2007.02.012

theoretical algorithms predicting the evolution of the interaction between the free cations and the network of the zeolites [22–24].

In general, zeolites are three-dimensional microporous crystalline solids with well-defined aluminosilicates structures. Their frameworks may contain linked cages, cavities or channels and are typically anionic. Guest cations can populate the pores to maintain its electrical neutrality and can participate to ion-exchange processes with other type of metals when it is in aqueous solution.

In the present work, we have initially used two types of zeolites which are the Faujasite knowing also as zeolite Y and the mordenite. They have respectively the following chemical formulas [25]:

$$|Na_{58}{}^{+}(H_2O)_{240}|[AI_{58}Si_{134}O_{384}]\text{-FAU},$$
$$|Na_8{}^{+}(H_2O)_{24}|[Al_8Si_{40}O_{96}]\text{-MOR}. \quad (1\text{-}1)$$

Fig. 1 gives their frameworks structures. In former works, chemicals synthesis method has been described [3,26–29].

Dues to their porosities and the simplicity of exchanging cations, zeolites can play a very important role in the manufacture of fuel cells membranes [30–32]. For this purpose, we were interested in studying the ionic conductivity of some cations in zeolite Y (ZY) and mordenite (M).

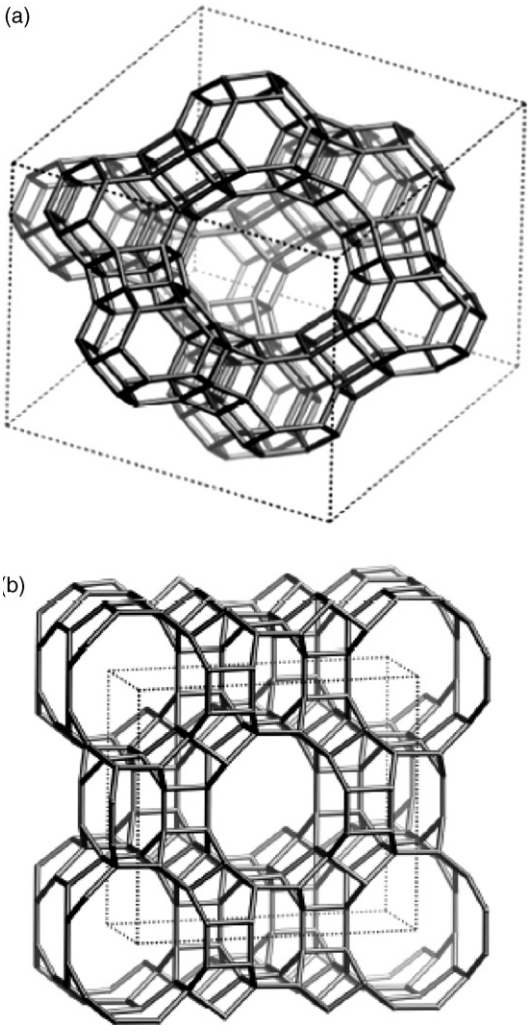

Fig. 1. (a) Framework of zeolite Y viewed along [1 1 1] direction and for (b) mordenite viewed along [0 0 1] direction.

Our choice was focused on the cobalt, copper, nickel and mixtures with low amounts of lithium which we estimated can bring improvements to the conduction.

In Section 2, a short description of the used devices and the different techniques of characterizations will be given. With ac impedance spectroscopy, ionic conductivity curves will be determined. And in the end, a discussion will be given referring to the effects of lithium on these samples.

2. Experimental

Ion-exchange of sodium cations Na^+ by others metallic cations like Co^{2+}, Cu^{2+}, Ni^+ or Li^+ was carried out in solution by conventional procedures. At ambient temperature, 1 g of the zeolite (ZY or M) was dissolved in 50 ml of metal chlorate solution and was stirred during 24 h. The exchange was performed as expected and carried out many times. After filtration, the solid was dried at 110 °C and the decanted liquid was analyzed by atomic absorption with AAS Vario6 Analytikjena equipment. The morphology of the powder zeolites, ZY and M, was observed with FEI Quanta 200 scanning electronic microscope (SEM) with X-ray analysis. Fig. 2 gives images for two different enlargement; the average grains dimensions is about 200 μm. Furthermore, the energy dispersive analysis of X-rays spectrum (EDAX) as seen by Fig. 3 gives the chemical compositions in a focused point of one grain of the samples. All the principle chemical elements of the zeolites exist with the guest cations.

The crystallographic zeolites structures was also been investigated by Philips X'Pert Pro X-Ray diffractometer (XRD). The good crystallinity for ZY sample was verified by the presence of the four 2θ reflections angles at 12.0°, 15.8°, 20.5° and 23.8°; and for the mordenite at 19.8°, 22.4°, 27.8°, 26.4°, 27.8° and 31.1°. Fig. 4 gives the X-ray pattern with the correspondent $h\,k\,l$ crystallographic Miller index.

During the thermal annealing, we have observed that only Co-ZY sample has underwent an important color modification from the pink color at the room temperature to the blue one at 700 °C. This is due to the different oxidations states of cobalt (+3, +2, 0 and −1). In addition, the presence of inter-crystalline water may permit to cobalt cations to be transformed to cobalt hydroxides. It has positive electric polarities able to guarantee the electrostatic neutrality inside the cavities of zeolites. The recent reference [33] can give an interesting explanation about the transformation of the colors of cobalt hydroxide. On other hand, we have checked that the X-ray spectrum of Co-ZY at 400 and at 700 °C stay representing a good crystallographic structure.

FTIR zeolites spectra were also given. Fig. 5 shows that the Co-ZY and Cu-M have roughly the same IR spectra with weak modifications towards lower frequencies.

Before proceeding with the conductivity measurement, the samples was powdered and encapsulated under a pressure of 10 t/cm^2 in small pellets of 13 mm of diameter and 1 mm of thickness. We have, also, evacuated the adsorbed water by heating the sample at 100 °C during 24 h. On the two faces of

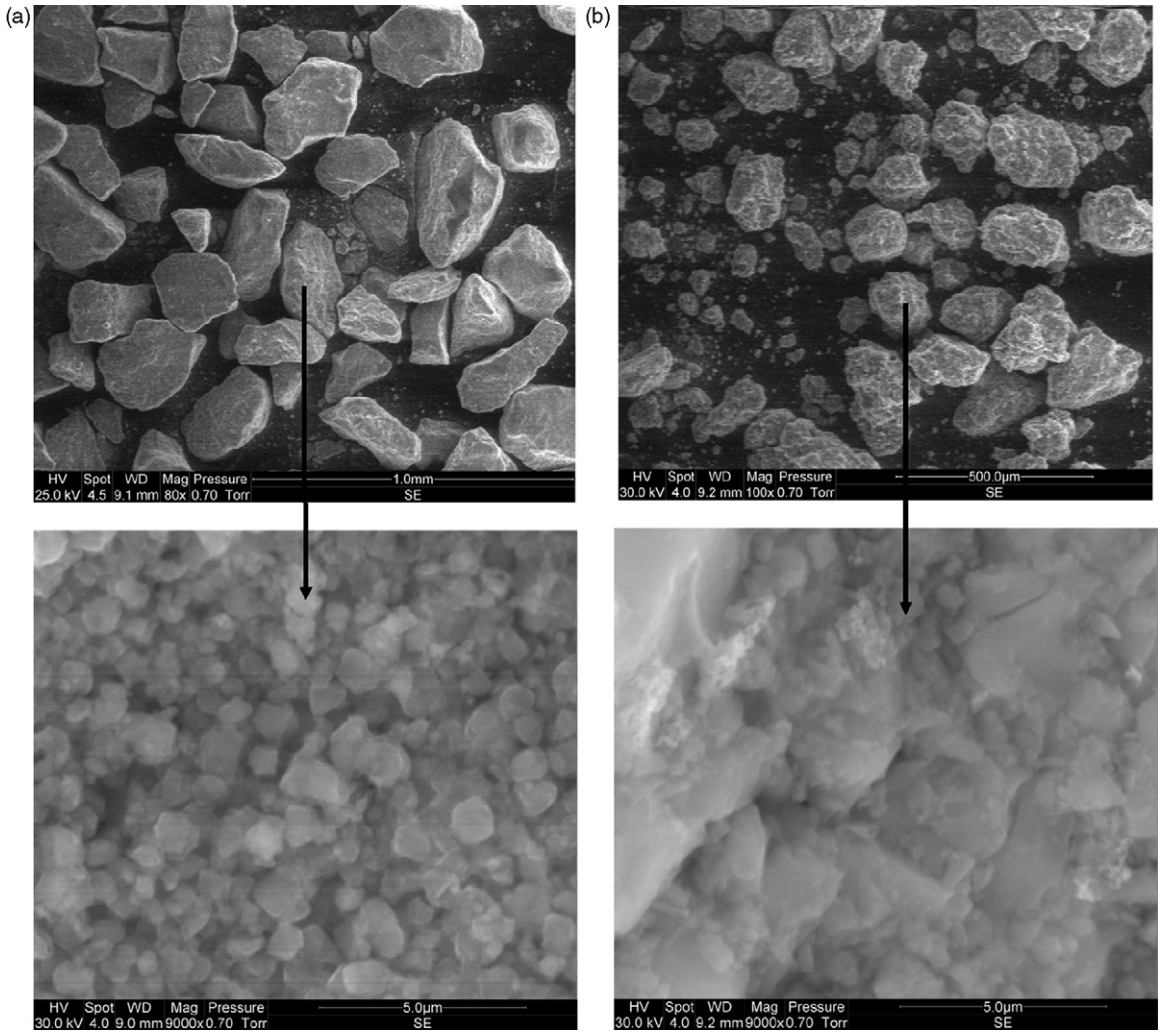

Fig. 2. SEM images of (a) Co^{2+}-ZY and (b) Cu^{2+}-M powder.

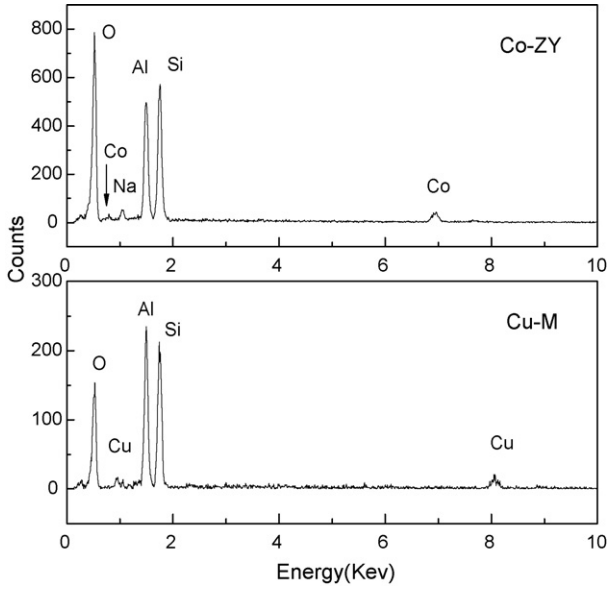

Fig. 3. The energy dispersive analysis of Co-ZY and Cu-M samples for HV = 25.0 and 30.0 kV

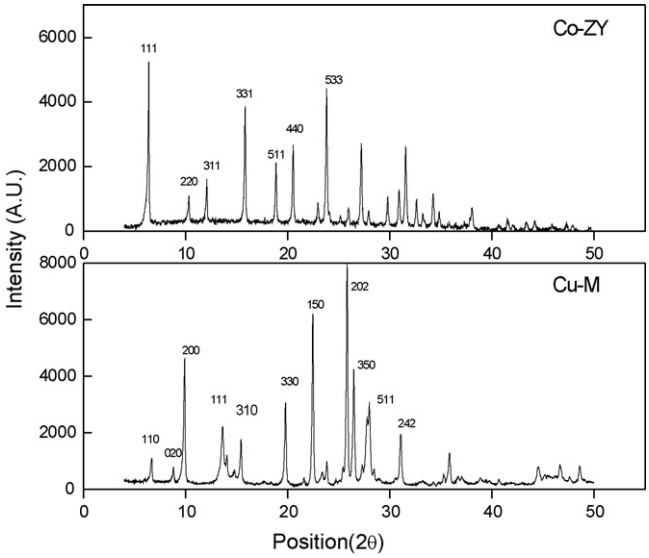

Fig. 4. XRD patterns of Co-ZY and Cu-M.

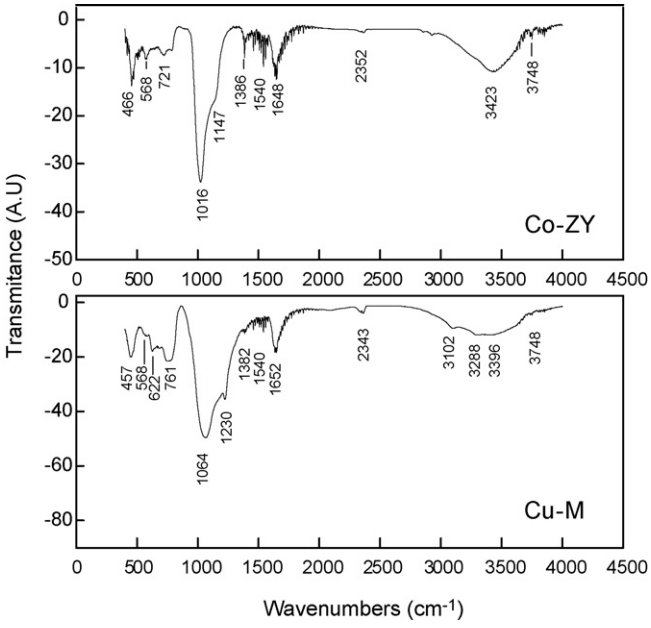

Fig. 5. FTIR spectrum of Co-ZY and Cu-M.

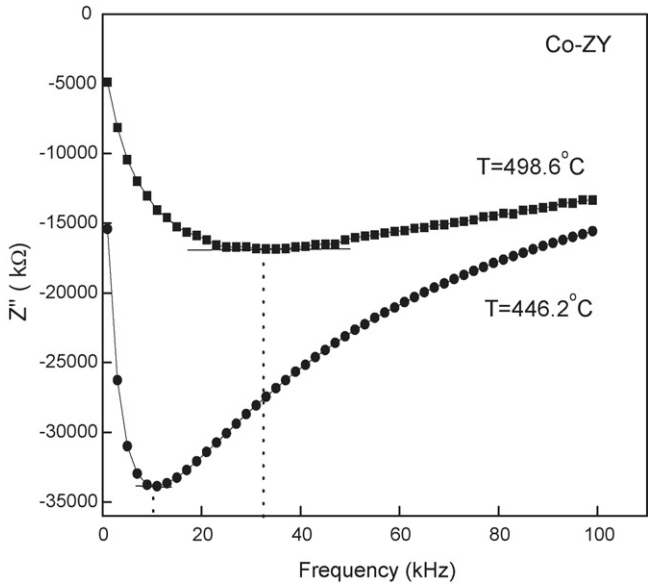

Fig. 6. Experimental complex impedance part of the Co-ZY sample vs. the frequency.

the pellets, a silver deposition and platinum wires was used to ensure the role of electrodes.

The impedance measurement was carried out by using a system including a standard analyzer of impedance type HP4192A which can sweep frequencies from 1 Hz to 13 MHz, a controller of temperature West Model 6100, a furnace with standard thermocouple K, an interface board GPIB, a computer with serial cable RS232 and a software Labview 4.0 for data acquisition.

3. Theory

The sample with his two electrodes was considered as a simple circuit formed by a resistance R parallel with a capacitance C and has the complex impedance versus frequency:

$$Z(\omega) - Z_0 = R\frac{1 - j(\omega/\omega_c)}{1 + (\omega/\omega_c)^2} \tag{3-1}$$

Z_0 is arbitrary complex impedance dependent of temperature and independent of the frequency and which will determine the shift of the conductivity arcs. The imaginary part of this impedance has a minimum at the following cut-off frequency:

$$\omega_c(T) = \frac{1}{RC} = \frac{\sigma(T)}{\varepsilon_0}. \tag{3-2}$$

It is related directly to the ionic conductivity coefficient $\sigma(T)$ dependant of absolute temperature and which has, for one type of carrier charges, the following form:

$$\sigma(T) = \sigma_0 \frac{T_0}{T} \exp\left[-\frac{E_a}{k}\left(\frac{1}{T} - \frac{1}{T_0}\right)\right] \tag{3-3}$$

where σ_0 is the ionic conductivity of the medium at a reference temperature T_0 and E_a is its activation energy.

4. Results and discussions

At the ambient temperature, all our samples are insulators for any passage of electric or ionic currents. They become ionic conductors in the neighborhoods of 400 °C. From this value to 650 °C and with suitable temperature steps, the displacements of the cut-off frequency were carefully measured. Fig. 6 gives the example of Co-ZY sample at two different temperatures, 446.2 and 498.6 °C. It shows a measurable displacement towards the higher frequencies. Combining these experimental results and theoretical expression (3-2), the conductivity curves versus the inverse of the absolute temperatures was determined. The corresponding Nyquist diagrams are arcs of circles having a shifted center as shown by Fig. 7.

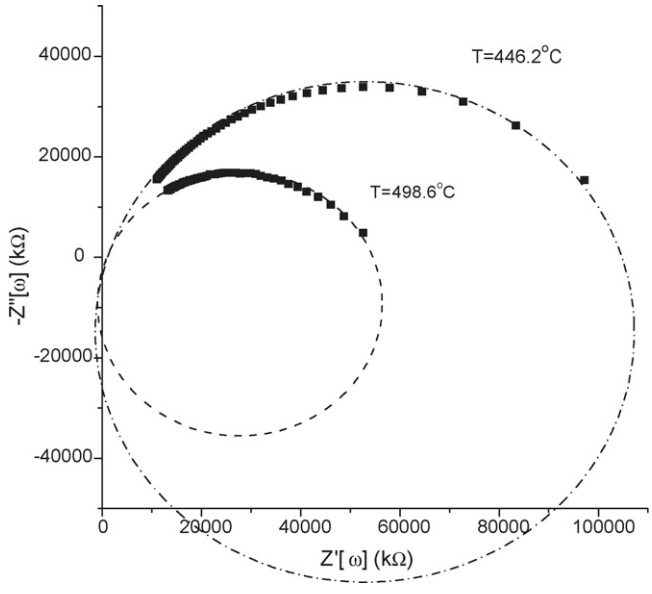

Fig. 7. Nyquist diagram of the zeolite Co-ZY sample.

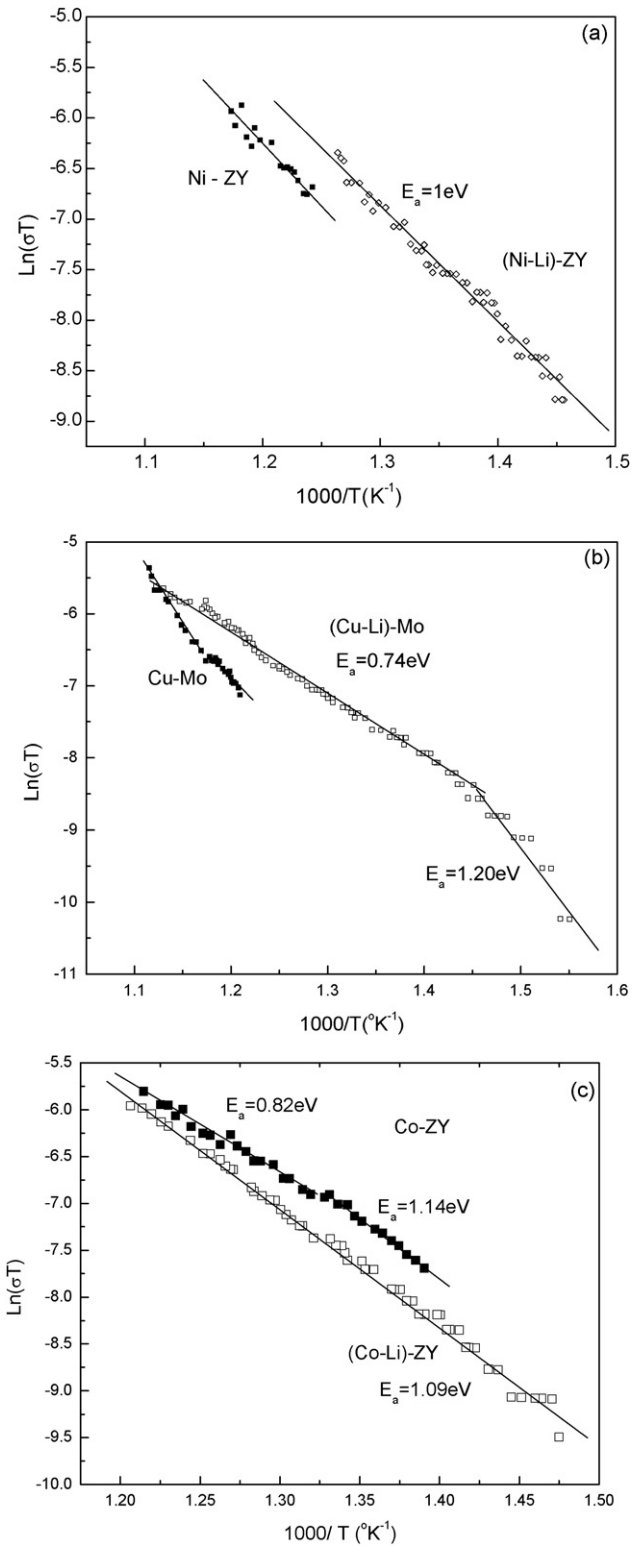

Fig. 8. Ionic conductivity curves of the samples: (a) Ni^+-ZY and (Ni^+–Li^+)-ZY (b) Cu^{2+}-M and (Cu^{2+}–Li^+)-M, (c) Co^{2+}–ZY and (Co^{2+}–Li^+)-ZY.

The first conductivity result is the outcome of nickel cations conduction. As presented by Fig. 8a, it has a high threshold temperature 530 °C from which it becomes conductor and has a significant conductivity ($\sigma = 1.45 \times 10^{-6}\ \Omega^{-1}\ m^{-1}$). The introduction of −0.03% of lithium, exchanged with nickel Ni^+, has shifted the conductivity curve to the lower temperature regions with a threshold temperature of 412 °C.

The same observations were obtained for the mordenite containing copper. Important displacements of the conductivity curve towards the lower temperatures were observed (Fig. 8b). The conductivity starts to be reasonable from 560 °C and with addition of ∼0.1% of lithium, the conductivity started from the lower temperature 370 °C. Break in this curve has also been observed around the critical temperature 415 °C. It corresponds certainly to the contribution of Cu^{2+} or to the couple (Cu^{2+}, Li^+) carrier charges on both sides of this temperature. Different results, than the preceding ones, were obtained for zeolite containing cobalt (Fig. 8c). The experimental conductivity curve shows that, in presence of ∼0.1% of lithium, a slight displacement towards the higher temperatures has taken place. In spite of this, the lithium has improved the threshold temperature from 450 to 405 °C and has given the curve a good linearity.

From these results, we have proved experimentally that the presence of lithium may play a significant role to improve ionic conduction and we also think that all these cations may be good traps for hydroxides and favorite the passage of protons in the zeolites matrix. Cobalt may be the best for this set of samples. We plan to continue this study for the research of better produced materials which may be employed as electrolytes for solid fuel cells.

5. Conclusion

We have proved experimentally that the conductivity depends essentially on the nature of cations encapsulated inside the pores of zeolites. The introduction of small quantity of lithium showed its efficiency in improving the curve of conductivity and moving it towards lower temperature zones. We think that these types of samples are suitable for the manufacturing of fuel cells membranes.

Acknowledgements

The authors would like to thank Dr. Mokhtar Ferid and Dr. R. Chtourou for heir helpful discussions. This work was supported by the Tunisian Ministry of Scientific Research and Technology and Competences Development.

References

[1] L. Li, B. Xue, J. Chen, N. Guan, F. Zhang, D. Liu, H. Feng, Appl. Catal. A: Gen. 292 (2005) 312–321.
[2] M.M. Mohamed, J. Mol. Catal. A: Chem. 211 (2004) 199–208.
[3] V.P. Valtchev, K.N. Bozhilov, J. Phys. Chem. B 108 (2004) 15587–15598.
[4] W.M. Meier, Z. Kristallogr. 115 (1961) 439.
[5] W.J. Mortier, Compilation of Extra Framework Sites in Zeolites, Butterworth, Guildford, 1982.
[6] N.F. Szarbo, H. Du, S.A. Ahmed Soliman, P.K. Dutta, Sens. Actuators B 82 (2002) 142–149.
[7] T. Arakawa, A. Kawabayashi, T. Saga, Sens. Actuators B 108 (2005) 899–902.
[8] M. Vilaseca, J. Coronas, A. Cirera, A. Cornet, J.R. Morante, J. Santamaria, Catal. Today 82 (2003) 179–185.

[9] N. Densakulprasert, L. Wannatong, D. Chotpattananont, P. Hiamtupa, A Sirivata, J. Schwankb, Mater. Sci. Eng. B 117 (2005) 276–282.
[10] J.-P. Li, T.-Z. Peng, C. Fang, Anal. Chim. Acta 455 (2002) 53–60.
[11] M.A. Zanjanchi, Sh. Sohrabnezhad, Sens. Actuators B 105 (2005) 502–507.
[12] G. Calzaferri, O. Bossart, D. Brühwiler, S. Huber, C. Leiggener, M.K. VanVeen, A.Z. Ruiz, C.R. Chim. 9 (2006).
[13] H.W. Langmi, A. Walton, M.M. Al-Mamouri, S.R. Johnson, D. Book, J.D. Speight, P.P. Edwards, I. Gameson, P.A. Anderson, I.R. Harris, J. Alloys Compd. 356–357 (2003) 710–715.
[14] I. Rosso, C. Galletti, G. Saracco, E. Garrone, V. Specchia, Appl. Catal. B: Environ. 48 (2004) 195–203.
[15] A.J. Hernández-Maldonado, F.H. Yang, G. Qi, R.T. Yang, Appl. Catal. B: Environ. 56 (2005) 111–126.
[16] V.S. Kambleand, N.M. Gupta, J. Phys. Chem. B 104 (19) (2000) 4588–4592.
[17] S. Li, C. Demmelmaier, M. Itkis, Z. Liu, R.C. Haddon, Y. Yan, Chem. Mater. 15 (14) (2003) 2687–2689.
[18] Y. Cao, T.T. Zhuang, J. Yang, H.D. Liu, W. Huang, J.H. Zhu, J. Phys. Chem. C 111 (2) (2007) 538–548.
[19] I. Othman, R.M. Mohamed, I.A. Ibrahim, M.M. Mohamed, Appl. Catal. A: Gen. 299 (2006) 95–102.
[20] S. Li, J. Sun, Z. Li, H. Peng, E.D. Gidley, T. Ryan, Y. Yan, J. Phys. Chem. B 108 (31) (2004) 11689–11692.
[21] G. Toussaint, L. Torcheux, J. Alzieu, J.C. Camps, D. Livigni, J.F. Sarrau, J.P. Vaurijoux, D. Benchetrite, V. Gauthier, M. Vilasi, J. Power Sources 144 (2005) 546–551.
[22] G. Maurin, P. Senet, S. Devautour, F. Henn, J.C. Giuntini, J. Non-Cryst. Solids 307–370 (2002) 1050–1054.
[23] G. Maurin, P. Senet, S. Devautour, P. Gaveau, F. Henn, V.E. Van Doren, J.C. Giuntini, J. Phys. Chem. B 105 (2001) 9297.
[24] G. Maurin, P. Senet, S. Devautour, F. Henn, J.C. Giuntini, V.E. Van Doren, Comput. Mater. Sci. 22 (1/2) (2001) 106.
[25] Ch. Baerlocher, Atlas of Zeolite Framework Types, fifth revised ed., Elsevier, Amsterdam (2001).
[26] M.M. Mohamed, T.M. Salama, I. Othman, I. Abd Ellah, Microporous Mesoporous Mater. 84 (2005) 84–96.
[27] S.-H. Lee, C.-H. Shin, G.J. Choi, T.-J. Park, I.-S. Nam, B. Han, S.B Hong, Microporous Mesoporous Mater. 60 (2003) 237–249.
[28] S.A Bagshaw, F. Testa, Microporous Mesoporous Mater. 42 (2001) 205–217.
[29] M.M. Mohamed, S.M.A Katib, Microporous Mesoporous Mater. 93 (2006) 71–81.
[30] P.V. Samant, J.B. Fernandes, J. Power Sources 125 (2004) 172–177.
[31] B. Libbya, W.H. Smyrla, E.L. Cusslera, AlChE J. 49 (4) (2003) 991–1001.
[32] V Tricoli, F. Nannetti, Electrochim. Acta 48 (2003) 2625–2633.
[33] R. Ma, Z. Liu, K. Takada, K. Fukuda, Y. Ebina, Y. Bando, T. Sasaki, Inorg. Chem. 45 (10) (2006) 3964–3969.